Spectral Target Detection at Twilight

Robert L. Sundberg
Spectral Sciences, Inc.
Burlington, MA, USA
e-mail: rob@spectral.com

***Abstract*— This paper will discuss the use of the Monte Carlo Scene (MCScene) code to simulate low light situations where the sun is near or below the horizon. MCScene is a high-fidelity model for full optical spectrum simulation. It provides an accurate, robust, and efficient means to generate spectral scenes for algorithm development and sensor trade studies. MCScene utilizes a Direct Simulation Monte Carlo (DSMC) approach for modeling 3D atmospheric radiative transfer including full treatment of molecular absorption and Rayleigh scattering, aerosol absorption and scattering, and multiple scattering. This paper will examine rare target detection statistics in simulated scenes as the sun moves from overhead to sunset and eventually to twilight.**

Keywords-scene simulation; target detection; hyperspectral; multispectral

I. INTRODUCTION

Improved simulations of hyperspectral and multispectral imagery (HSI and MSI) under low illumination conditions are required to keep pace with the improved imaging capabilities of spectral imaging sensors, see for example imagery from BlackSky [1]. The MCScene code is a high-fidelity spectral image simulation capability [2], [3], that is based on a DSMC approach for modeling the 3D radiative transport. The code has been enhanced to allow treatment of long atmospheric path simulations such as those found under twilight conditions and highly off-nadir or near horizontal viewing geometries [4].

In this paper, we report on the initial results in a study on sub-pixel spectral target detection under low light conditions. Reflective boundary planes implemented in MCScene allows the code to simulate long path length scenes such as those encountered in limb viewing sensors or scenes where the sun is very low on the horizon or even below the horizon, twilight conditions. In Section II, we present some imagery simulated for three scene showing the low illumination simulations capabilities of MCScene. In Section III, we examined detection statistics for subpixel targets embedded in the simulated scenes as a function of solar zenith angle. Conculsions for the paper are presented in Section IV.

II. LOW ILLIMINATION SCENE SIMULATIONS

An example of low illumination simulation is shown in Figure 1. This figure shows a series of simulations for a sensor at 20 km altitude looking due west with a 45° slant angle as the sun sets over Fort Collins, CO. The simulation requires a reflectance map and a Digital Elevation Map (DEM), we used a Landsat based reflectance map and downloaded the DEM from the USGU site [5]. A mid-latitude summer atmosphere was used along with a rural aerosol, as defined in MODTRAN [6]. The RGB bands of the simulation are shown for solar zenith angles of 30, 45, 60 and 70 degrees. Note the color change as the scene coloring shifts toward the red as the sun sets. When the sun is below the mountain peaks only photons which undergo multiple scattering can illuminate the shadowed ground.

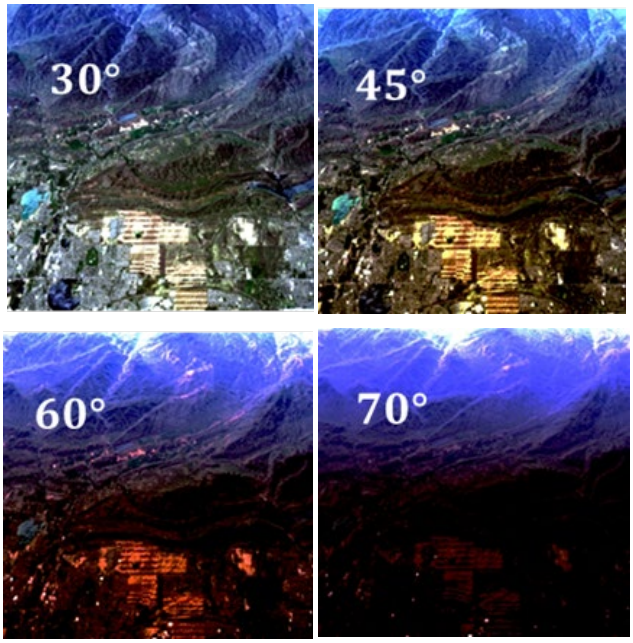

Figure 1. Linear stretched RGB radiance images simulated by MCScene for a Fort Collins, CO for solar zenith angles of 30, 45, 60 and 70 degrees.

In another example, a mountain ridge was used to cast a shadow over part of the Rochester Institute of Technology (RIT) Center for Imaging Sciences collected scene of Cook City, MT [7]. Figure 2 shows the RGB radiance images for a series of simulations with solar zenith angles of 0, 80, and 90 degrees. With a solar zenith angle of 80 degrees the scene is fully in shadow. The MCScene simulations were performed with an observer placed at 20 km altitude viewing nadir.

The final example shows a scene derived from a 1999 AVIRIS data collect over a Boreal region in Saskatchewan, Canada [8]. We have resampled the spectral imagery to match the 126 spectral bands of the HyMap sensor [9] to speed up the spectral simulations, which scale linearly with the number of spectral bands. Figure 3 shows a linear stretch of the RGB radiance images for a subset of the Boreal scene

for solar zenith angles of 45 and 90 degrees. These scenes were simulated for a sensor at 20 km altitude looking nadir with very low aerosol loading with a resulting visibility of 100 km. The image at 90-degrees solar zenith shows additional noise but much of the spectral content appears present even when the scene radiance is down by nearly four orders of magnitude.

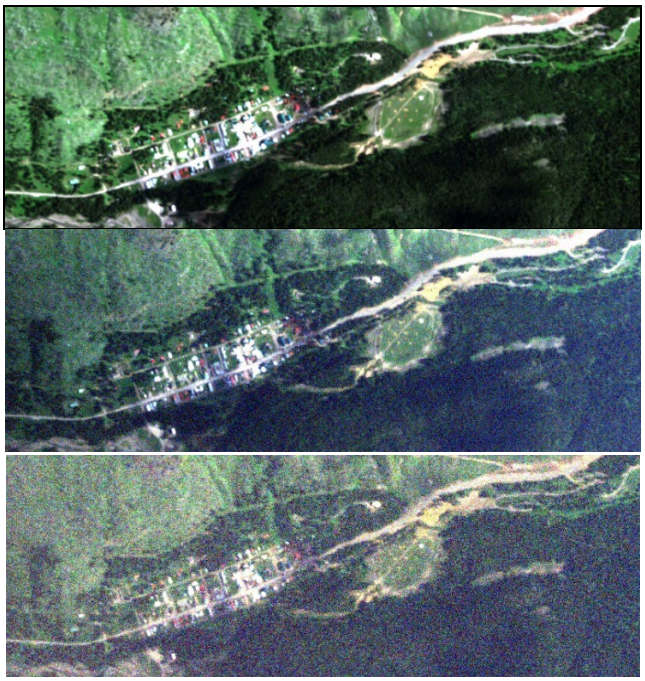

Figure 2. Linear stretched RGB radiance images simulated by MCScene for a subset of the RIT Target Detection Blind-Test scene for solar zenith angles of 0 (top), 80 and 90 (bottom) degrees.

Figure 3. Linear stretched RGB radiance images simulated by MCScene for a subset of the Boreal scene for solar zenith angles of 45 (top) and 90 (bottom) degrees.

III. TARGET DETECTION RESULTS

The scenes in Figures. 2 and 3 have been atmospherically compensated to scene reflectance using the in-scene code QUAC [10]. The standard Adaptive Coherence Estimator (ACE) [11] detector was then used to evaluate detection performance for the scenes using a pure target reflectance signature. For the scene shown in Figure 2, Figure 4 shows the Receiver-Operator Curves (ROC) for the detection of 400 subpixel targets varying from a fill-factor of 2% to 10%. Targets make up fewer than 0.18% of the pixels in the scene, perhaps most importantly the scene covariance can be calculated without significant impact from the targets that are present. There is decreased target detection performance for scenes with lower illumination primarily due to the increased importance of the scene noise as the illumination decreases. The spectral at sensor radiance at sunset is approximately four orders of magnitude below the signal when the scene is fully sunlit, but 80% of the targets are still detected with a false alarm rate of 10^{-2} [12].

Figure 5 shows the ROC plots for the Boreal scene with the same embedded subpixel target as was used in the Blind-Test scene. In this figure we plot the detection rate for solar zeniths of 0, 45 and 90 degrees for the high visibility simulations. We have also added a curve for the detection results for a 90-degree solar zenith angle case with a visibility of 23 km, labeled hazy in the figure. The detection results improve as the visibility is lowered from 100 km to 23 km. This result may seem counter intuitive, but the additional aerosol leads to more scattering which in this scenario increase the number of photons reaching the ground, thus improving the detection results. Figure 6 shows the linearly stretched RGB image for the 23 km visibility case. Examination of the detailed spectral data across these

two 90-degree solar zenith scenes indicates that the additional scattering tends to increase the radiance in the NIR and SWIR part of the spectrum. The blue target spectrum has a significant SWIR feature which would be more easily detected with the enhanced SWIR radiance. This specific result is very dependent on the target spectral signature and its contrast to the scene elements.

IV. CONCLUSIONS AND FUTURE WORK

In this paper, we report initial results for an ongoing study of rare spectral target detection statistics under low light conditions. To explore this problem a first-principles simulation model for spectral imagery was used. This model is based on a DSMC radiative transport approach. The code, named MCScene, has been successfully validated through comparisons with exact scattering calculations, and its utility has been demonstrated in applications to remote sensing problems. Recent upgrades to MCScene allow simulation of low light and twilight conditions. Subpixel spectral targets were embedded in the scene reflectance maps before simulating the scene radiance under different illumination conditions. The low light simulations indicate that target detection even under twilight conditions is possible given sufficient sensor signal to noise and target to background spectral contrast.

ACKNOWLEDGMENT

The authors wish to acknowledge Spectral Sciences, Inc. for support under an internal research and development grant.

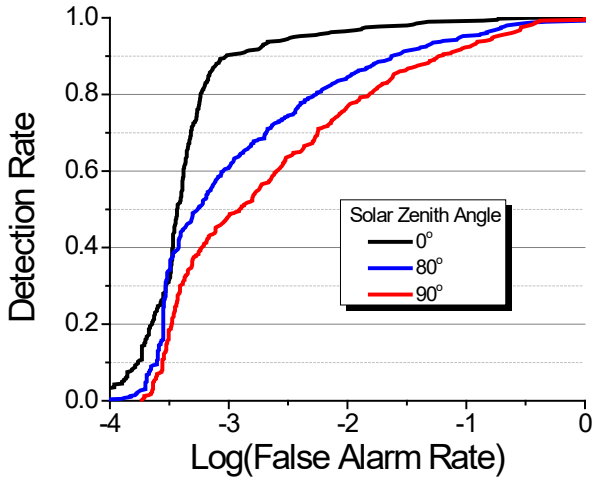

Figure 4. ROC curves for blue roof subpixel targets in the RIT Blind-Test Scene simulated by MCScene using QUAC atmospheric correction followed by the ACE detection algorithm.

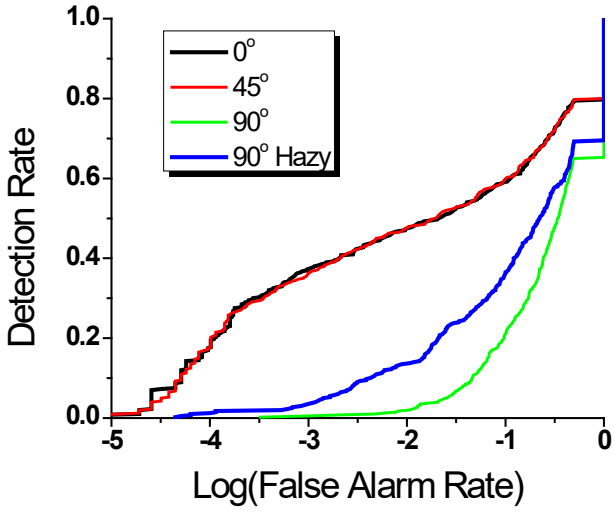

Figure 5. ROC curves for blue roof subpixel targets detected in the Boreal scene simulated by MCScene after QUAC atmospheric correction followed by the ACE detection algorithm.

Figure 6. Linear stretched RGB radiance image simulated by MCScene for a subset of the Boreal scene for solar zenith angles of 90 degrees and a visibility of 23 km.

REFERENCES

[1] K. Kirschner, https://payloadspace.com/blacksky-reports-q1-results, accessed: 2024-03-31

[2] S. Richtsmeier, A. Berk, S. M. Adler-Golden, and L. S. Bernstein, "A 3D Radiative-Transfer Hyperspectral Image Simulator for Algorithm Validation," Proceedings of ISSSR 2001, Quebec City, Canada (June 2001).

[3] S. Richtsmeier, R. L. Sundberg, R. Haren, and F. O. Clark, "Fast Monte Carlo Full Spectrum Scene Simulation," Proc. SPIE 6233, (2006).

[4] A. Berk, S. Richtsmeier and R. Sundberg, "Limb-viewing hyperspectral image simulation based on a polygonal earth cross-section (PEX) model," 2017 IEEE International Geoscience and Remote Sensing Symposium (IGARSS), Fort

Worth, TX, USA, 2017, pp. 1449-1452, doi: 10.1109/IGARSS.2017.8127239.

[5] USGS, https://apps.nationalmap.gov/downloader, accessed: 2024-04-01

[6] A. Berk, et al., "MODTRAN6: a major upgrade of the MODTRAN radiative transfer code," Proc. SPIE, Algorithms and Technologies for Multispectral, Hyperspectral, and Ultraspectral Imagery XX, 90880H (June 13, 2014); doi:10.1117/12.2050433.

[7] J. P. Kerekes and D.K. Snyder, "Unresolved target detection blind test project overview," Proc. of SPIE Vol. 7695 769521-1 (2010).

[8] R. Green, et al., "AVIRIS Land-Surface Mapping in Support of the Boreal Ecosystem-Atmosphere Study," 2000-01-012, https://ntrs.nasa.gov/citations/20020014837, accessed: 2024-04-01.

[9] T. Cocks, R. Jenssen, A. Stewart, I. Wilson, and T. Shields, 1998, "The HyMap Airborne Hyperspectral Sensor: The System, Calibration and Performance," Proc. 1st EARSeL Workshop on Imaging Spectroscopy (M. Schaepman, D.Schläpfer, and K.I. Itten, Eds.), 6-8 October 1998, Zurich, EARSeL, Paris, pp. 37-43.

[10] L. S. Bernstein, X. Jin, B. Gregor, and S. Adler-Golden, "The Quick Atmospheric Correction (QUAC) code: algorithm description and recent upgrades," Opt. Eng. 51(11), 111719 (2012). doi:10.1117/1.OE.51.11.111719

[11] S. S. Kraut, L. L. Scharf, and R. W. Butler, "The Adaptive Coherence Estimator: A uniformly most-powerful invariant adaptive detection statistic," IEEE Trans. Signal Processing, Vol. 53, No. 2 (2005).

[12] R. L. Sundberg "The impact of topographic shadows on subpixel target detection", Proc. SPIE 12688, Imaging Spectrometry XXVI: Applications, Sensors, and Processing, 1268803 (20 October2023), doi:10.1117/12.2675427